THE JOURNAL OF PHYSICAL CHEMISTRY C

Article

pubs.acs.org/JPCC

Lattice Monte Carlo Simulations in Search of Zeolite Analogues: Effects of Structure Directing Agents

Mohammad Navaid Khan,[†] Scott M. Auerbach,*[,‡] and Peter A. Monson*[,†]

[†]Department of Chemical Engineering and [‡]Department of Chemistry, University of Massachusetts Amherst, Amherst, Massachusetts 01003, United States

Supporting Information

ABSTRACT: We use parallel tempering Monte Carlo simulations to search for crystalline states of a lattice model of silica polymerization in the presence of structure directing agents (SDAs). Following previous work where we have discretized continuous space into a body-centered cubic (bcc) lattice, we have modeled tetrahedral molecules ($T(OH)_4$) as corner-sharing tetrahedra on a bcc unit cell. The SDAs were represented as quasi-spherical species with diameters of 6.4 and 10.4 Å to study the effect of SDA size on the resulting crystal structures. Our parallel tempering Monte Carlo simulations produce fully connected crystalline structures finding the emergence of 3D microporous materials with SDAs occupying the pore spaces and 2D layered materials with SDAs occupying the gallery space in between layers. We have found that the strength of SDA−oxygen attraction plays a significant role in directing final micropore structures. For relatively strong attractions (>1.2 kcal/mol SDA−oxygen contacts) we have found only 2D layered materials; for attractions below this cutoff we observed 3D microporous crystals; and for no attraction—modeling the SDA as a quasi-hard sphere—we again found only 2D layered materials. In the space of 3D microporous crystals, we have also found that using larger SDAs or a lower concentration of a given SDA generate crystals with larger rings.

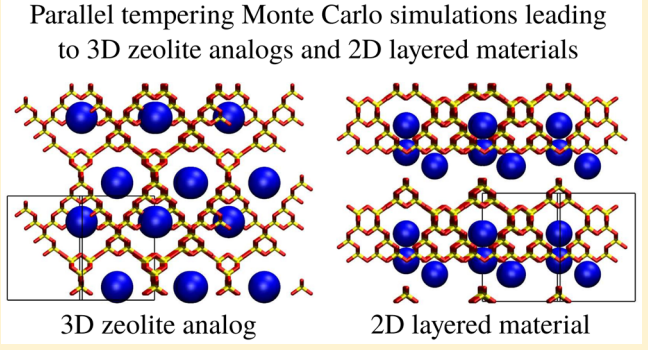

1. INTRODUCTION

Zeolites are microporous crystalline aluminosilicates that enjoy a multitude of commercial applications in catalysis, adsorption, and membrane separations.[1] At present, over 200 zeolite framework types have been identified;[2] however, only a handful have been utilized commercially.[1] Zeolites are typically produced via hydrothermal synthesis using silica and alumina sources in the presence of structure directing agents (SDAs), which promote the formation of microporous crystals as evident by the presence of SDAs in the resulting micropores.[3,4] The design of zeolites for novel applications through the control of micropore size/shape and crystal size/shape has been a topic of great interest[5] with emphasis on elucidating the roles of SDA species in the self-assembly process.[6] However, experimental characterization methods are not yet able to generate atomic-level resolution of silica−SDA structures on length scales characteristic of zeolite critical nuclei (5−10 nm).[7] Molecular modeling methods[8,9] are thus well poised to complement experimental characterization by providing atomic-level information on the roles of SDA species during zeolite crystallization. In the present work, we perform parallel tempering Monte Carlo simulations of a model of silica polymerization in the presence of various SDA species to investigate how SDA properties influence the resulting micropore structures.

Several studies have been reported to elucidate the role of SDAs in the process of synthesizing zeolites and other pure-silica ordered materials.[3,4,10−13] Important control parameters in the synthesis process include composition of the initial mixture, Si/Al ratio, pH, temperature, and type and concentration of SDA. Gies and Marler[14] argued that it is not straightforward to separately study the influences of pH and cationic SDAs on zeolite formation because the cations are accompanied by a charge balancing species, commonly OH^-, which also changes the initial solution pH. To disentangle these effects, Gies and Marler studied silica crystallization in the presence of various neutral SDAs in aqueous solutions, varying the size, shape, and chemical character of the SDAs. They observed that changing the chemical character of the SDA, from nonpolar to polar to hydrogen bonding, does not bring any change in the resulting cage structure, suggesting that silica micropore self-assembly is principally governed by silica−SDA van der Waals interactions. They also observed that increasing SDA size results in crystals with larger cages, with SDAs present in each cage. Lobo et al.[13] summarized the final microporous silica structures obtained from a wide variety of SDAs observing

Received: September 28, 2015
Revised: November 16, 2015
Published: November 18, 2015

DOI: 10.1021/acs.jpcc.5b09450
J. Phys. Chem. C 2015, 119, 28046−28054

that increasing the sizes of linear and branched SDAs produce larger pores in both 1-D and 3-D zeolites, respectively. However, a more complete understanding of the effects of SDAs during the crystallization process is still lacking because characterization methods do not as yet provide atomic-level information on the dynamics of the process. In such cases, molecular modeling methods may provide valuable insights into the synthesis process.[8,9]

Molecular modeling of zeolite nucleation requires the treatment of a complex mix of physical interactions such as solvation, charge balancing, and hydrophobic effects, along with chemical interactions such as silica polymerization, acid−base equilibria, and heteroatom energetics—all simulated for relatively long lengths and times with efficient sampling methods that can handle potentially glassy systems.[8] No single model has yet to include all these effects, explaining why simulating zeolite nucleation remains such a daunting target. In 1996, Lewis et al. reported a simulation study of a library of SDAs optimized in known zeolite frameworks to predict new SDAs for making target zeolites based on host−guest stabilities.[15] This seminal study established the approach of optimizing host−guest interactions of putative SDAs in known zeolite frameworks, which can suggest new SDAs but says little about how zeolites actually form. More recently, Burton et al.[16] reported energy optimization of various quaternary organic amines in known high-silica zeolites to elucidate thermodynamic factors that control the eventual zeolite phases found in synthesis experiments.[1,2] They found that piperidine derivatives have a better fit with the pear-shaped cage of AEI, whereas polycyclic quaternary ammonium compounds fit better inside the cylindrical shaped cage of CHA framework. Although such studies provide valuable atomic level details of the process, they do not give information on pathways leading to the formation of zeolite crystals.

Lewis et al. extended their study to force-field-based optimizations of silica fragments likely to play a role in zeolite formation,[17] testing the stabilities of open-framework silica fragments in the absence and presence of hydration and SDAs. They found that both charged and neutral SDAs are essential for stabilizing hydrated, open-framework silica fragments, hence corroborating the findings of Gies and Marler[14] that silica−SDA van der Waals interactions are central to the formation of micropores. More recently, Van Santen and co-workers performed classical molecular dynamics[18] and *ab initio* molecular dynamics[19] to study the stabilities of silica−tetraalkylammonium cation clusters, finding that the cavities in silica oligomers are stabilized by the alkyl chains in tetraalkylammonium SDAs, again pointing to the importance of silica−SDA van der Waals interactions. Despite this important progress in our understanding of silica−SDA clusters, the computational costs of these methods restrict the systems to relatively small sizes and short simulations times and hence do not provide pathways that proceed all the way to microporous crystal structures.

The development of efficient models and sampling of silica polymerization has been crucial for enhanced understanding of silica material synthesis. Wu and Deem developed and applied a Monte Carlo approach[20] for modeling silica polymerization, cluster formation, and nucleation. They estimated the nucleation barrier for silica crystallization to be on the order of $10^2 k_B T$ and the critical nucleus size to be ∼50 silica units. Several groups have reported simulation approaches for predicting libraries of hypothetical zeolites,[21−26] furnishing millions of new target structures for synthetic zeolite chemists. However, these simulations usually follow topological rules, hence deviating from actual molecular pathways of zeolite formation. More recently, Pophale et al.[27] developed a novel simulation method for predicting the synthesis of SDAs from a given set of reagents and reactions, which may be useful making a target zeolite. SDA selection was performed following the method of Lewis et al.,[15] based on host−guest stability simulations between putative SDAs and the target zeolite. This method was experimentally verified by Schmidt et al.[28] where they developed an SDA for synthesizing the STW zeolite framework. Although this approach is computationally efficient in generating SDAs for a given framework, it remains unclear how changing properties of the SDA would result in a different micropore structure.

Lattice models provide computational efficiency by discretizing continuous space into countable configurations, thereby allowing the sampling of longer lengths and time scales. Such discrete models have been successful in predicting the structures of micellar solutions[29−33] and surfactant−silica systems.[34] Recently our group reported a body-centered cubic (bcc) lattice model of silicic acid to study silica polymerization to amorphous nanoparticles and gels at the isoelectric point of silica (pH ∼ 2)[35] and across pH values and silica concentrations.[36] This bcc lattice model is inspired by periodic DFT calculations on various dense all-silica polymorphs,[37] showing that the cohesive energy per unit SiO_2 is remarkably uniform across this class of systems, varying only by about 10 kJ/mol SiO_2. Jin et al. subsequently expanded their lattice model to include surfactant self-assembly to study the formation of MCM-41 mesoporous silica, finding evidence for cooperative silica−surfactant mesoscale assembly.[38] While the lattice model approach makes the study of these systems more computationally accessible, the lattice constrains allowed structures that can form during the simulations. For instance, the T−O−T bond angles accessible in the lattice model are more restricted than those seen in nature. Nevertheless, the studies described above demonstrate the power of lattice models to elucidate the properties of disordered systems, raising the question whether such lattice models may shed light on crystal structures as well.

Specialized molecular simulation methods are required to surmount free energy barriers separating amorphous and ordered phases of a given material. Such methods break up into the following two classes: kinetic approaches such as transition-path sampling[39,40] and forward-flux sampling,[41,42] which build up accurate pictures of free energy barriers and dividing surfaces separating amorphous and ordered phases by sampling kinetically relevant pathways;[43] and thermodynamic methods such as parallel tempering Monte Carlo (PTMC),[44,45] which may bypass free energy barriers to efficiently sample free energy minima associated with amorphous and ordered phases. PTMC accomplishes this by simulating several system replicas at various temperatures and attempting swaps of configurations between replicas in accord with detailed balance, thereby simulating heating/cooling cycles that efficiently move simulations between amorphous and ordered states. Jin et al. recently applied PTMC to study the bcc lattice model of silica to examine the feasibility of using PTMC to identify dense and microporous crystalline phases of this model. Jin et al. initiated all PTMC simulations from disordered states and demonstrated that PTMC can be used to generate a rich array of crystalline structures such as zeolite analogues, chalcogenides, and two-

DOI: 10.1021/acs.jpcc.5b09450
J. Phys. Chem. C 2015, 119, 28046−28054

dimensional layered materials with this simple bcc lattice model.[46] Although these PTMC simulations do not necessarily follow kinetically relevant pathways as discussed above, they provide a way forward toward future studies of zeolite nucleation. In particular, these PTMC calculations were performed in the absence of SDAs, raising the question of how the presence and properties of SDAs may influence the microporous structures that emerge in these simulations. In the present work, we extend the PTMC simulations of this bcc lattice model of silica by incorporating SDAs to study their effects on final microporous crystal structures. Our particular focus is on SDA size, concentration, and interaction with silica species. The SDA is modeled below as a quasi-spherical species with excluded volume and van der Waals-like, near-neighbor attractions to silica oxygens. We find that silica polymerization in the presence of bigger SDAs results in zeolites with larger rings, and higher concentrations of SDAs lead to zeolites with smaller rings. We also find a relatively narrow range of silica−SDA attraction values that lead to 3D microporous materials.

The remainder of this paper is organized as follows: in section 2 we discuss the model and its parameters; in section 3 we describe the Monte Carlo simulation technique; section 4 presents our results on the effects of SDA concentration, size, and attraction strength on crystal structure; and finally in section 5, we present a summary of our results and concluding remarks on future research implied by the findings in this article.

2. MODEL

Our model extends the work of Jin et al.,[35] where three-dimensional continuous space is discretized onto a body-centered cubic (bcc) lattice. A tetrahedral molecule ($T(OH)_4$) is represented in a bcc unit cell with the tetrahedral (T) atom located at the body-center of the unit cell and the hydroxyl groups (−OH) located at four of the eight vertices, as shown in Figure 1a. This model has been applied to study silica polymerization[35] at the isoelectric point of silica (pH ∼ 2)[47] and the self-assembly zeolite analogues.[46] The SDAs are modeled below as quasi-spheres by imposing far-neighbor repulsions from a single lattice site, as shown in Figure 1b. We consider two SDA sizes as summarized in Table 1: a medium SDA with a diameter of 6.4 Å, which excludes 59 bcc sites, and a large SDA with a diameter of 10.4 Å, excluding 181 bcc sites. We have recently applied this silica−SDA lattice model to study silica polymerization to amorphous nanoparticles and gels for various pH values and silica concentrations.[36] In general, we make the approximation of treating the solvent as vacancies on the lattice, as we have consistently done in our earlier work.[48]

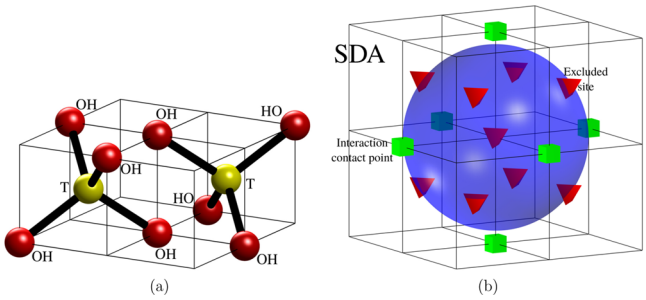

Figure 1. Representation of different species on the bcc lattice. (a) $T(OH)_4$ molecules with T atom at the center of the unit cell and oxygen atoms located on the vertices. (b) An SDA molecule as a single site with far neighbor repulsions; here SDA diameter is 3.2 Å. Red tetrahedra represents excluded sites and green cubes represent attraction contact points.

Table 1. Simulation Parameters Studied in This Work

variable	description	values
TO_4 concentration (TO_4/box)	tetrahedral units in simulation	32, 40, 48, 56
SDA concentration (SDAs/box)	low	2
	high	4
SDA diameter (Å)	medium	6.4
	large	10.4
SDA−$T(OH)_4$ attraction	$\varepsilon_{O-SDA} = f\varepsilon_{T(OH)_4-T(OH)_4}$	$f = 0.1n$, $n = 1, 2, 3, ..., 10$

With three species in our model—SDA, $T(OH)_4$, and solvent—there can be a total of six interactions energies. As in our earlier work,[48] we have set the reference energy scale to be the condensation energy between adjacent tetrahedral molecules, $\varepsilon_{T(OH)_4-T(OH)_4}$. In a condensation reaction, the hydroxyl groups from two tetrahedra come together (via allowed double occupancy by hydroxyl groups) to create a bridging oxygen which liberates a water molecule, represented as a new vacancy on the lattice created by the allowed double occupancy[35] (see Figure 2a). Each condensation reaction is assumed to change the total system energy by $\varepsilon_{T(OH)_4-T(OH)_4} = -4$ kcal/mol,[35,49] representing the exothermicity of silica condensation, one of the driving forces for silica network formation. We prohibit the formation of two-membered rings as those would have a high angular strain.[50] As such, all fully connected silica networks that can form in our bcc lattice model exhibit the same energy per $T(OH)_4$, broadly consistent with periodic DFT results for dense and zeolitic silica polymorphs.[37] This also indicates that silica−SDA interactions will determine the eventual crystalline ground states of this silica−SDA lattice model.

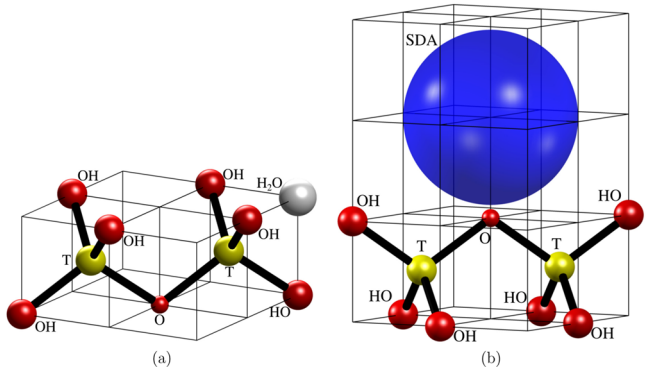

Figure 2. Type of interactions in the system: (a) condensation reaction between two $T(OH)_4$ molecules; (b) near-neighbor attraction between bridging oxygen and SDA molecule.

We model attractions between SDAs and $T(OH)_4$ tetrahedra according to the spirit of van der Waals interactions, following the work of Gies and Marler,[14] Lewis et al.,[17] and van Santen and co-workers.[18,19] In particular, for each SDA size, we allow attractions to bridging oxygens at sites just beyond the region of excluded volume (see Figure 2b). We do not allow SDA−$T(OH)_4$ attractions to terminal OH groups because we focus on van der Waals type and not highly polar, attraction types in

DOI: 10.1021/acs.jpcc.5b09450
J. Phys. Chem. C 2015, 119, 28046−28054

this work. For each medium/large SDA there are 6/48 possible SDA−O attraction sites (see Table 1). For each attraction site we posit an attraction strength of $\varepsilon_{O-SDA} \leq 0$; we vary ε_{O-SDA} over 11 values $f \times \varepsilon_{T(OH)_4-T(OH)_4}$ where f takes the values (0, 0.1, 0.2, 0.3, 0.4, 0.5, 0.6, 0.7, 0.8, 0.9, and 1.0), to determine how the strength of SDA−$T(OH)_4$ interactions influences final crystal structures. Below we show specific results for the cases f = 0.2 and 1.0; the remaining results are given in the Supporting Information. Table 1 summarizes all systems studied.

To complete the specification of our model, we note that SDA−SDA interactions are assumed to be hard sphere in nature. In addition, all interactions with solvent (vacancies) are neglected for computational simplicity, consistent with our previous development of this lattice model.[35,48]

3. SIMULATION METHODOLOGY

We have applied parallel tempering Monte Carlo simulations[44,45] (PTMC) to study crystalline states of silica in the presence of SDA species. The scaled temperature of the lattice model ($T^* = k_BT/\varepsilon_{T(OH)_4-T(OH)_4}$) corresponding to ambient conditions has been estimated to be 0.15 using a previous silica solubility analysis.[35] PTMC simulates multiple copies of the system, each with a different temperature, and attempts configurational swaps between (typically adjacent) replicas with probabilities that obey detailed balance within the canonical ensemble. We have used room temperature (T^* = 0.15) as the lowest temperature in our PTMC temperature grid, which contained 50 temperatures for all PTMC simulations reported below. We have chosen the highest PTMC temperature to produce a largely dissolved state wherein the majority of $T(OH)_4$ units are unpolymerized; our previous study indicates that T^* = 0.30 is suitable for the PTMC maximum temperature.[46] Temperature grid spacing was determined such that the acceptance probability of exchange between adjacent replicas is close to 20%.[51] This was achieved by running short Monte Carlo simulations of 5000 steps and refining the temperature grid to the point where the average acceptance probability is around 20%. We performed PTMC simulations in a parallel implementation using the message passing interface (MPI) protocol.

We have implemented the following three kinds of canonical ensemble Monte Carlo moves (along with replica exchange moves): translations, rotations, and swaps. A translation move is made where any molecule, among SDAs and $T(OH)_4$ tetrahedra, is selected at random and is attempted to be moved to any vacant site on the lattice. A rotational move is where a random $T(OH)_4$ molecule is selected and is attempted to be rotated to the other four vertices in the corresponding bcc unit cell. The third kind of move is a swap where a $T(OH)_4$ tetrahedron and an SDA are selected at random, and an exchange is attempted between their positions. The acceptance probabilities for these moves are based on the Metropolis criterion.[52] One Monte Carlo "step" comprises N translations, N rotations, and N swaps, where N is the total number of molecules in the system. Exchanges between configurations are attempted every 5000 MC steps. Ninety percent of such exchanges are attempted between adjacent temperature configurations, and 10% of the exchanges are attempted by randomly selecting temperatures that lie within a quarter length of the temperature grid. The acceptance probability of exchanging configurations at temperatures T_1 and T_2 with energies E_1 and E_2, respectively, is given by[44]

$$\min\left[1, \exp\left\{\left(\frac{1}{k_BT_1} - \frac{1}{k_BT_2}\right)(E_1 - E_2)\right\}\right]$$

We have simulated a cubic lattice of size 8 × 8 × 8 unit cells with periodic boundary conditions for 10×10^6 MC steps. The system length scale is defined by the Si−O bond length of 1.6 Å, which sets the length of the simulation box to be 14.8 Å. Table 1 shows the TO_4 concentration that has been studied in this work. For comparison, the dense silica polymorph β-cristobalite contains 64 $T(OH)_4$ tetrahedra in this simulation box.[46]

We have studied SDAs with two sizes as listed in Table 1—the diameter of the medium size SDA is 6.4 Å with 59 excluded sites and 6 SDA−O interaction contacts. Whereas the diameter of the larger SDA is 10.4 Å, slightly greater than the ionic diameter of tetrapropylammonium cation (9.0 Å[53]), with 181 excluded sites and 48 SDA−O interaction contacts. We studied 11 values of the parameter ε_{O-SDA}, and we considered SDA concentrations of either 2 or 4 SDAs per simulation cell, giving a total number of 44 distinct systems studied (see Table 1 for a detailed summary), each simulated at 50 temperatures on the PTMC grid. These simulations produced 10 distinct crystalline microporous structures with three-dimensional connectivity and another roughly 10 two-dimensional layered materials. The layered materials that form in our simulations are all composed of fully connected (i.e., all Q_4) silica, in contrast to many synthesized layered materials that are stabilized by terminal silanols. Because of the stochastic nature of these simulations, a consistent final structure is not always observed at each of the temperature values on the PTMC grid. However, to study the effects of SDA size, and SDA concentration on the final structure, the most frequently occurring structures on the PTMC grid were selected. All the structures discovered through this materials discovery platform are shown in the Supporting Information, including the conditions found in our PTMC simulations that produced each material.

We have characterized the materials resulting from our simulations based on their ring size distributions (RSD), where the ring size is defined as the total number of T atoms present in a given ring. We have used the R.I.N.G.S. package[54] to compute the total number of primitive rings[55] in each crystal structure.

4. RESULTS AND DISCUSSION

Here we show the results of several PTMC simulations of silica polymerization around SDAs with various SDA concentrations, sizes, and interaction strengths to determine how SDA properties influence final silica crystalline structures. In particular, we have studied the influence of SDA concentration by considering 2 and 4 SDAs per simulation cell for both medium (M) and large (L) SDAs, giving the following four systems: 2M, 2L, 4M, and 4L. We found in our PTMC simulations that the 4L system produces exclusively partially condensed two-dimensional layered structures, while we are predominantly interested in studying three-dimensional microporous networks characterized by their distribution of rings (ring-size distribution or RSD). As such, we show below 2 and 4 M systems (with $\varepsilon_{O-SDA} = 0.2 \times \varepsilon_{T(OH)_4-T(OH)_4}$) to study the effect of SDA concentration on RSDs; we then show the comparison between 2 M and 2L systems (same ε_{O-SDA} value) to study the effect of SDA size on RSDs. Finally, we show PTMC results for the 2 M system with $\varepsilon_{O-SDA}/\varepsilon_{T(OH)_4-T(OH)_4}$ =

DOI: 10.1021/acs.jpcc.5b09450
J. Phys. Chem. C 2015, 119, 28046−28054

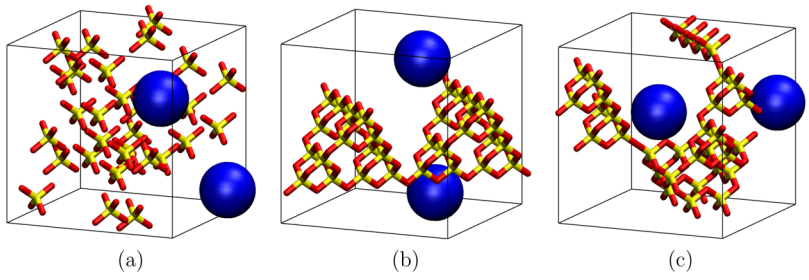

Figure 3. Snapshots during PTMC with $T^* = 0.15$, 32 $T(OH)_4$, 2 medium SDAs ($D_{SDA} = 6.4$ Å), and $\varepsilon_{O-SDA} = 0.2\varepsilon_{T(OH)_4-T(OH)_4}$: (a) initially random configuration; (b) two-dimensional material observed after 2×10^6 MC steps; (c) three-dimensional microporous crystal observed after 10×10^6 MC steps.

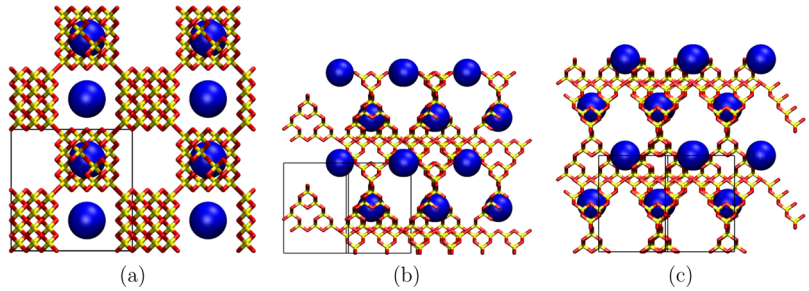

Figure 4. The $2 \times 2 \times 2$ periodic extension of Figure 3c showing SDAs in the micropores: (a) plane ⟨001⟩; (b) plane $\langle\bar{1}10\rangle$; (c) plane ⟨110⟩.

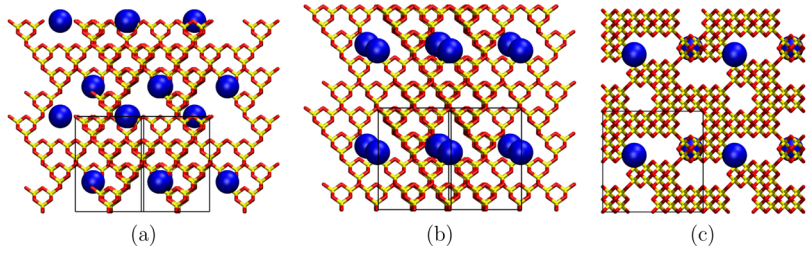

Figure 5. Microporous crystalline material observed with 48 $T(OH)_4$ and 2 medium SDAs ($D_{SDA} = 6.4$ Å), shown as $2 \times 2 \times 2$ periodic extension of the simulation box: (a) plane ⟨011⟩; (b) plane ⟨101⟩; (c) plane ⟨100⟩.

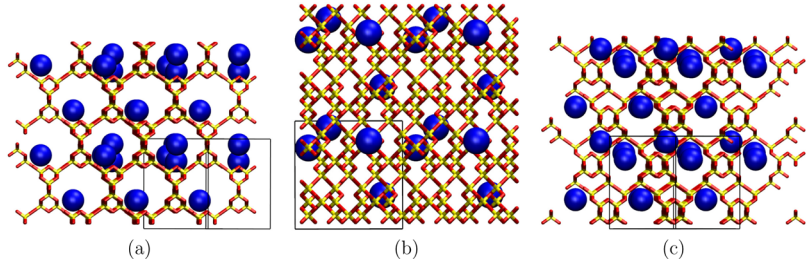

Figure 6. Microporous crystalline material observed with 48 $T(OH)_4$ and 4 medium SDAs ($D_{SDA} = 6.4$ Å), shown as $2 \times 2 \times 2$ periodic extension of the simulation box: (a) plane $\langle\bar{1}10\rangle$; (b) plane ⟨100⟩; (c) plane ⟨110⟩.

1.0 to investigate the effect of SDA interaction strength. The crystalline frameworks obtained for all other systems are given in the Supporting Information.

We begin by illustrating various configurations from a PTMC simulation at $T^* = 0.15$ with 32 $T(OH)_4$, 2 medium SDAs ($D_{SDA} = 6.4$ Å), and $\varepsilon_{O-SDA} = 0.2\varepsilon_{T(OH)_4-T(OH)_4}$ (see Figure 3). The simulation began by placing all species at random locations on the lattice, as shown in Figure 3a. Figure 3b shows the emergence of a two-dimensional layered material, observed after 2×10^6 MC steps. In such a configuration, all tetrahedra are fully condensed and the SDAs occupy the space between the layers. The maximum SDA−O interaction contacts per SDA is 1 for this 2D material. Figure 3c provides a system snapshot after 10×10^6 MC steps, where we observe a three-dimensional microporous crystal. In this configuration the maximum number of SDA−O interaction contact per SDA is 4, which is lower in energy than the 2D structure, making it the thermodynamically favorable configuration. A $2 \times 2 \times 2$ periodic extension of this material is shown in Figure 4 from three perspectives, revealing that the SDAs are present inside the micropores. This particular framework was not observed in the absence of SDA molecules,[46] which suggests that the presence of these SDAs has directed the formation of this framework.

DOI: 10.1021/acs.jpcc.5b09450
J. Phys. Chem. C 2015, 119, 28046−28054

Effect of SDA Concentration. We have observed that decreasing the TO_4 concentration keeping SDA concentration fixed has the same effect on RSD as that of increasing the SDA concentration keeping TO_4 units fixed. Therefore, in this work we only discuss the effect of change in SDA concentration. Here we compare 2 and 4 medium SDA systems ($\varepsilon_{O-SDA} = 0.2 \times \varepsilon_{T(OH)_4-T(OH)_4}$) to study the effects of SDA concentration on RSDs. Figures 5 and 6 show the microporous frameworks that arise from PTMC simulations with 2 and 4 medium SDAs, respectively. In Figure 7 we show the ring size distributions for

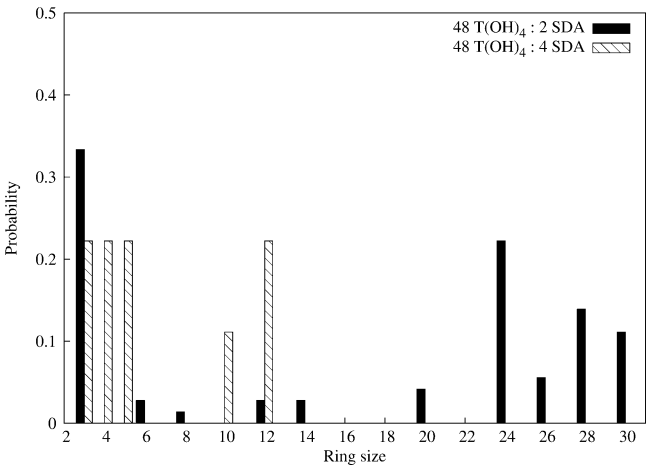

Figure 7. Ring size distributions for micropore structures shown in Figure 5 (2 medium SDAs) and Figure 6 (4 medium SDAs), showing that increasing SDA concentration produces frameworks with smaller rings to optimize SDA−$T(OH)_4$ attractions.

both structures. Figure 7 shows that silica polymerization around 2 medium SDAs produces rather large rings containing in excess of 18 T atoms; these are likely artifacts of the bcc lattice model. Figure 7 also shows that increasing the SDA concentration to 4 medium SDAs produces a microporous framework with smaller rings, all with 12 or fewer T atoms. We rationalize this trend in terms of the assembly of frameworks that optimize SDA−O contacts, considering that all fully connected silica networks exhibit the same silica energy in our model. Having more SDAs in the simulation cell provides the opportunity for lowering the system energy by building microporous frameworks with more such SDA−O contacts. Indeed, the average SDA−O interaction contacts increase from 4 to 16 for 2 and 4 medium SDAs, respectively. This increase in average contacts result in the formation of a more compact microporous framework in Figure 6 with smaller rings than those in Figure 5.

Effect of SDA Size. Here we show the comparison of microporous frameworks that arise from PTMC with 2 medium SDAs (6.4 Å) and 2 large SDAs (10.4 Å), respectively, as shown in Figures 5 and 8. The ring size distributions for these two frameworks are shown in Figure 9, which once again shows

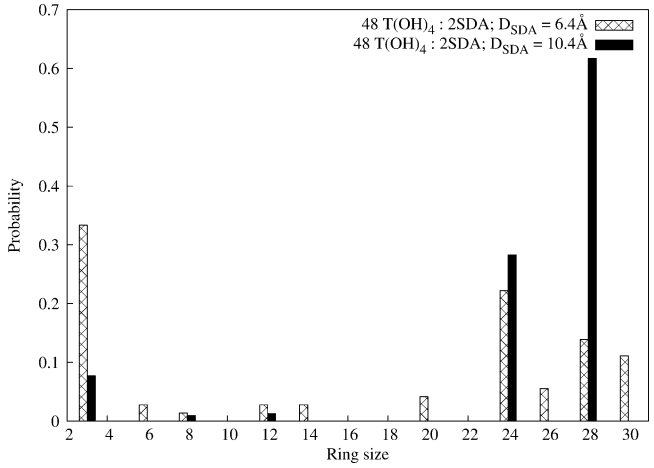

Figure 9. Ring size distributions for micropore structures shown in Figure 5 (2 medium SDAs) and Figure 8 (2 large SDAs), showing that increasing SDA size produces a framework with fewer smaller rings and more large rings, driven by the combination of molecular fit and optimizing SDA−O attractions.

rather larger rings in both structures. Figure 9 shows qualitatively that using the larger SDA pushes the ring size distribution to deplete smaller rings in favor of larger ones. While this finding—that bigger SDAs produce more large rings—makes intuitive sense from the standpoint of templating and molecular fit, we can analyze these results from an energetic standpoint as well. In particular, we find that the average SDA−O interaction contact is 4 for micropore structure for with medium SDA (Figure 5) and is 24 for the structure formed around the large SDA (Figure 8). Such a change in SDA−O interaction contacts is consistent with that seen above when changing SDA concentration. However, while increasing SDA concentration and size both lead to increased SDA−O contacts, such enhanced attractions lead to opposite trends in ring size: smaller rings for higher SDA concentration and larger rings for larger SDA size. These model predictions are qualitatively consistent with the experimental findings of Gies and Marler,[14] who found in the synthesis of pure-silica caged materials that using larger SDAs produces materials with larger rings and cages. It will be interesting to see if this general trend holds in our future studies with structured SDAs.

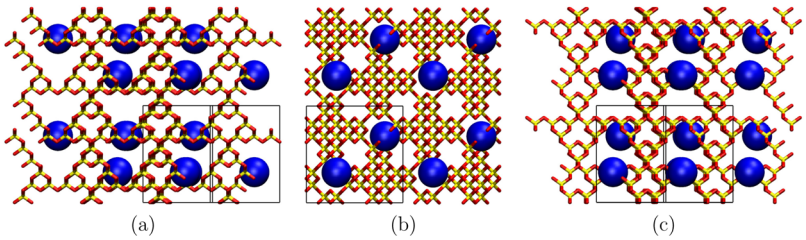

Figure 8. Microporous crystalline material observed with 48 $T(OH)_4$ and 2 large SDAs (D_{SDA} = 10.4 Å), shown as 2 × 2 × 2 periodic extension of the simulation box: (a) plane ⟨$\bar{1}$01⟩; (b) plane ⟨100⟩; (c) plane ⟨101⟩.

DOI: 10.1021/acs.jpcc.5b09450
J. Phys. Chem. C 2015, 119, 28046−28054

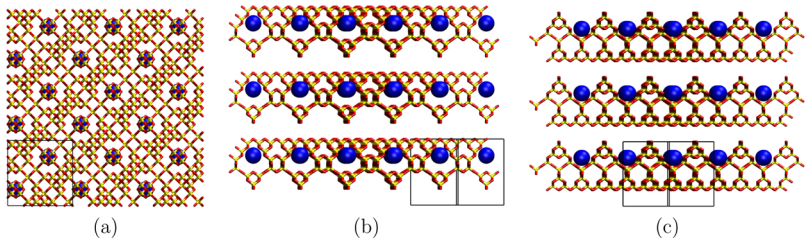

Figure 10. Perspectives of ordered, layered material arising from PTMC with strong silica−SDA attractions ($\varepsilon_{O-SDA} = \varepsilon_{T(OH)_4-T(OH)_4}$) with 2 medium SDAs (6.4 Å) and 48 $T(OH)_4$: (a) plane ⟨001⟩; (b) plane $\langle\bar{1}10\rangle$; (c) plane ⟨110⟩.

Effect of Silica−SDA Attraction Strength. Here we discuss PTMC simulation results from varying silica−SDA attraction strength through the parameter ε_{O-SDA}, which was varied over 11 values of $f \times \varepsilon_{T(OH)_4-T(OH)_4}$ (f = 0, 0.1, 0.2, 0.3, 0.4, 0.5, 0.6, 0.7, 0.8, 0.9, and 1.0). Below we show results with 2 medium SDAs from the extreme case of f = 1; the remaining results are shown in the Supporting Information. Figure 10 shows that PTMC with very strong silica−SDA attractions ($\varepsilon_{O-SDA} = \varepsilon_{T(OH)_4-T(OH)_4}$, i.e., f = 1) produces a two-dimensional layered material with SDAs positioned in the galleries between silica layers, in analogy with the structures of pillared clays.[56] In general, we have observed that three-dimensionally connected microporous materials arise in our PTMC simulations only in a relatively narrow range of silica−SDA attractions, characterized by $0 < |\varepsilon_{O-SDA}| \leq 0.3|\varepsilon_{T(OH)_4-T(OH)_4}|$; for stronger attractions such as those in Figure 10 we observe only layered materials. Although the average SDA−O interaction contact per SDA is 5, the SDA is strongly attracted to oxygens, making the 2D materials in Figure 10 the thermodynamic stable state. This transition from 3D to 2D architectures with increasing $|\varepsilon_{O-SDA}|$ is driven by the optimization of silica−SDA attractions via flattened pore structures. We note that in the particularly interesting case of ε_{O-SDA} = 0, in which the SDA species act simply as hard quasi-spheres, PTMC produces only layered materials, implying that silica−SDA attractions are essential for the formation of fully connected microporous frameworks. We find it remarkable that there is such a relatively narrow range of such attractions—a "Goldilocks" scenario—that produces 3D microporous materials.

5. SUMMARY AND CONCLUSIONS

In this work we have applied PTMC simulations to search for crystalline states of a lattice model of silica polymerization in the presence of structure directing agents (SDAs). Consistent with our previous work, we have modeled silica monomers $[Si(OH)_4]$ as corner-sharing tetrahedra in the bcc unit cell, with each Si atom at the body center and OH groups on one of two possible sets of tetrahedral vertices. SDAs were modeled as quasi-spheres with diameters of 6.4 and 10.4 Å. To mimic silica−SDA van der Waals interactions, silica−SDA attractions are allowed in lattice sites just outside the region of SDA excluded volume. Silica polymerization is represented through condensation processes, modeled through the double occupancy by terminal OH groups producing a new bridging oxygen. We have implemented parallel tempering Monte Carlo with a grid of 50 temperatures, allowing these simulations to pass efficiently from disordered initial silica−SDA conditions to crystalline silica materials with structures driven in part by the properties of the SDAs. We have varied SDA concentration, size, and attraction strength to silica to determine how these SDA properties affect the final crystalline silica structures.

These PTMC simulations have produced 3D microporous materials and 2D layered materials with SDAs occupying the pore and gallery spaces, respectively. We observed 3D microporous materials that were not found in the absence of SDAs, suggesting a structure directing affect in our simulations. We have observed more 2D structures than 3D structures over the temperature range studied, which may suggest that there could be more pathways leading to 2D structures than those leading to 3D in our model. We have discovered a remarkably narrow range of silica−SDA attraction values (≤1.2 kcal/mol SDA−oxygen contacts) that produces 3D microporous materials. Otherwise, for either no silica−SDA attraction or too strong an attraction, 2D layered materials were obtained from PTMC. When considering only 3D microporous materials, we have found that decreasing SDA concentration and increasing SDA size both lead to materials with smaller rings shifted to larger rings in the ring size distributions, driven in our simulations by optimization of silica−SDA attractions.

This simulation study raises many intriguing avenues for future work. We plan to compare our present results from quasi-spherical SDAs to those for structured SDAs such as tetraalkylammonium species, whose tetrahedral structures are easily accommodated on the bcc lattice. Through such comparisons we may discover the effects of SDA structure on micropore structure. We also plan to compare our PTMC results—which may not follow kinetically relevant pathways—to those from methods such as forward-flux sampling[41,42] to determine the nature of kinetically relevant pathways and if such pathways may produce different micropore crystalline structures. Such a comparison will begin to suggest whether all-silica zeolite formation is principally controlled by thermodynamics or kinetics. Although the present study does not yet answer the question as to how all-silica zeolites crystallize, our present results do provide an important direction forward for answering such an important question. Such studies will represent a significant step forward in understanding the synthesis of crystalline microporous materials such as all-silica zeolites.

■ ASSOCIATED CONTENT

Supporting Information

The Supporting Information is available free of charge on the ACS Publications website at DOI: 10.1021/acs.jpcc.5b09450.

Structures observed from our calculations—both 2D and 3D—and the conditions that generated them (PDF)

DOI: 10.1021/acs.jpcc.5b09450
J. Phys. Chem. C 2015, 119, 28046−28054

AUTHOR INFORMATION

Corresponding Authors

*E-mail: auerbach@chem.umass.edu (S.M.A.).
*E-mail: monson@ecs.umass.edu (P.A.M.).

Notes

The authors declare no competing financial interest.

ACKNOWLEDGMENTS

This work was supported by a grant from U.S. Department of Energy (Contract DE-FG02-07ER46466). Moreover, the computational resources for this research were provided by Massachusetts Green High Performance Computing Center (MGHPCC).

REFERENCES

(1) Auerbach, S. M.; Carrado, K. A.; Dutta, P. K. *Handbook of Zeolite Science and Technology*; Dekker: New York, 2003.

(2) Baerlocher, C.; McCusker, L. B.; Olson, D. H. *Atlas of Zeolite Framework Types*; Elsevier: Amsterdam, 2007.

(3) Davis, M. E.; Lobo, R. Zeolite and Molecular-Sieve Synthesis. *Chem. Mater.* **1992**, *4*, 756−768.

(4) Davis, M. E. Zeolites from a Materials Chemistry Perspective. *Chem. Mater.* **2014**, *26*, 239−245.

(5) Barton, T. J.; Bull, L. M.; Klemperer, W. G.; Loy, D. A.; McEnaney, B.; Misono, M.; Monson, P. A.; Pez, G.; Scherer, G. W.; Vartuli, J. C.; Yaghi, O. Tailored Porous Materials. *Chem. Mater.* **1999**, *11*, 2633−2656.

(6) Moliner, M.; Rey, F.; Corma, A. Towards the Rational Design of Efficient Organic Structure-Directing Agents for Zeolite Synthesis. *Angew. Chem., Int. Ed.* **2013**, *52*, 13880−13889.

(7) Davis, T.; Drews, T.; Ramanan, H.; He, C.; Dong, J.; Schnablegger, H.; Katsoulakis, M.; Kokkoli, E.; McCormick, A.; Penn, R.; Tsapatsis, M. Mechanistic Principles of Nanoparticle Evolution to Zeolite Crystals. *Nat. Mater.* **2006**, *5*, 400−408.

(8) Auerbach, S. M.; Ford, M. H.; Monson, P. A. New Insights Into Zeolite Formation from Molecular Modeling. *Curr. Opin. Colloid Interface Sci.* **2005**, *10*, 220−225.

(9) Auerbach, S. M.; Fan, W.; Monson, P. A. Modelling the Assembly of Nanoporous Silica Materials. *Int. Rev. Phys. Chem.* **2015**, *34*, 35−70.

(10) Shvets, O. V.; Kasian, N.; Zukal, A.; Pinkas, J.; Cejka, J. The Role of Template Structure and Synergism Between Inorganic and Organic Structure Directing Agents in the Synthesis of UTL Zeolite. *Chem. Mater.* **2010**, *22*, 3482−3495.

(11) Zones, S. I.; Burton, A. W.; Lee, G. S.; Olmstead, M. M. A Study of Piperidinium Structure-directing Agents in the Synthesis of Silica Molecular Sieves under Fluoride-based Conditions. *J. Am. Chem. Soc.* **2007**, *129*, 9066−9079.

(12) Wagner, P.; Nakagawa, Y.; Lee, G.; Davis, M.; Elomari, S.; Medrud, R.; Zones, S. Guest/Host Relationships in the Synthesis of the Novel Cage-Based Zeolites SSZ-35, SSZ-36, And SSZ-39. *J. Am. Chem. Soc.* **2000**, *122*, 263−273.

(13) Lobo, R. F.; Zones, S. I.; Davis, M. E. Structure-Direction in Zeolite Synthesis. *J. Inclusion Phenom. Mol. Recognit. Chem.* **1995**, *21*, 47−78.

(14) Gies, H.; Marler, B. The Structure-Controlling Role of Organic Templates for the Synthesis of Porosils in the System SiO_2/Template/H_2O. *Zeolites* **1992**, *12*, 42−49.

(15) Lewis, D. W.; Willock, D. J.; Catlow, C. R. A.; Thomas, J. M.; Hutchings, G. De novo Design of Structure-Directing Agents for the Synthesis of Microporous Solids. *Nature* **1996**, *382*, 604−606.

(16) Burton, A.; Lee, G.; Zones, S. Phase Selectivity in the Syntheses of Cage-based Zeolite Structures: An Investigation of Thermodynamic Interactions Between Zeolite Hosts and Structure Directing Agents by Molecular Modeling. *Microporous Mesoporous Mater.* **2006**, *90*, 129−144.

(17) Lewis, D. W.; Catlow, C. R. A.; Thomas, J. Application of Computer Modelling to the Mechanisms of Synthesis of Microporous Catalytic Materials. *Faraday Discuss.* **1997**, *106*, 451−471. General Discussion Meeting on Solid State Chemistry - New Opportunities from Computer Simulations, Univ. Coll. London: London, England, June 30−July 02, 1997.

(18) Szyja, B. M.; Hensen, E. J. M.; van Santen, R. A. Retro-Analysis of Silicate Aggregation in Pentasil Zeolite Formation. *Catal. Today* **2011**, *169*, 156−166.

(19) Szyja, B. M.; Vassilev, P.; Trinh, T. T.; van Santen, R. A.; Hensen, E. J. M. The Relative Stability of Zeolite Precursor Tetraalkylammonium-Silicate Oligomer Complexes. *Microporous Mesoporous Mater.* **2011**, *146*, 82−87.

(20) Wu, M.; Deem, M. Monte Carlo Study of the Nucleation Process During Zeolite Synthesis. *J. Chem. Phys.* **2002**, *116*, 2125−2137.

(21) Li, Y.; Yu, J.; Liu, D.; Yan, W.; Xu, R.; Xu, Y. Design of Zeolite Frameworks with Defined Pore Geometry Through Constrained Assembly of Atoms. *Chem. Mater.* **2003**, *15*, 2780−2785.

(22) Treacy, M.; Rivin, I.; Balkovsky, E.; Randall, K.; Foster, M. Enumeration of Periodic Tetrahedral Frameworks. II. Polynodal Graphs. *Microporous Mesoporous Mater.* **2004**, *74*, 121−132.

(23) Li, Y.; Yu, J.; Wang, Z.; Zhang, J.; Guo, M.; Xu, R. Design of Chiral Zeolite Frameworks with Specified Channels Through Constrained Assembly of Atoms. *Chem. Mater.* **2005**, *17*, 4399−4405.

(24) Rivin, I. Geometric Simulations - A Lesson from Virtual Zeolites. *Nat. Mater.* **2006**, *5*, 931−932.

(25) Deem, M. W.; Pophale, R.; Cheeseman, P. A.; Earl, D. J. Computational Discovery of New Zeolite-Like Materials. *J. Phys. Chem. C* **2009**, *113*, 21353−21360.

(26) Pophale, R.; Cheeseman, P. A.; Deem, M. W. A Database of New Zeolite-like Materials. *Phys. Chem. Chem. Phys.* **2011**, *13*, 12407−12412.

(27) Pophale, R.; Daeyaert, F.; Deem, M. W. Computational Prediction of Chemically Synthesizable Organic Structure Directing Agents for Zeolites. *J. Mater. Chem. A* **2013**, *1*, 6750−6760.

(28) Schmidt, J. E.; Deem, M. W.; Davis, M. E. Synthesis of a Specified, Silica Molecular Sieve by Using Computationally Predicted Organic Structure-Directing Agents. *Angew. Chem., Int. Ed.* **2014**, *53*, 8372−8374.

(29) Larson, R. Self-Assembly of Surfactant Liquid-crystalline Phases by Monte Carlo Simulation. *J. Chem. Phys.* **1989**, *91*, 2479−2488.

(30) Mackie, A.; Panagiotopoulos, A.; Szleifer, I. Aggregation Behavior of a Lattice Model for Amphiphiles. *Langmuir* **1997**, *13*, 5022−5031.

(31) Widom, B. Lattice Model of Microemulsions. *J. Chem. Phys.* **1986**, *84*, 6943−6954.

(32) Chen, K.; Ebner, C.; Jayaprakash, C.; Pandit, R. Microemulsions in Oil-water-surfactant Mixtures - Systematics of a Lattice-Gas Model. *Phys. Rev. A: At., Mol., Opt. Phys.* **1988**, *38*, 6240−6254.

(33) Woo, H.; Carraro, C.; Chandler, D. Assembly of Extended Interfaces and Micelles: Charge Frustrated Models of Amphiphilic Mixtures. *Faraday Discuss.* **1996**, *104*, 183−191. General Discussion on Complex Fluids at Interfaces, Univ. Cambridge, Churchill Coll., Cambridge, England, Sept 18−20, 1996.

(34) Siperstein, F.; Gubbins, K. Phase Separation and Liquid Crystal Self-assembly in Surfactant-inorganic-solvent Systems. *Langmuir* **2003**, *19*, 2049−2057.

(35) Jin, L.; Auerbach, S. M.; Monson, P. A. Modeling Three-dimensional Network Formation with an Atomic Lattice Model: Application to Silicic Acid Polymerization. *J. Chem. Phys.* **2011**, *134*, 134703.

(36) Khan, M. N.; Auerbach, S. M.; Monson, P. A. Lattice Model for Silica Polymerization: Monte Carlo Simulations of the Transition between Gel and Nanoparticle Phases. *J. Phys. Chem. B* **2014**, *118*, 10989−10999.

(37) Astala, R.; Auerbach, S.; Monson, P. Density Functional Theory Study of Silica Zeolite Structures: Stabilities and Mechanical Properties of SOD, LTA, CHA, MOR, and MFI. *J. Phys. Chem. B* **2004**, *108*, 9208−9215.

DOI: 10.1021/acs.jpcc.5b09450
J. Phys. Chem. C 2015, 119, 28046−28054

(38) Jin, L.; Auerbach, S. M.; Monson, P. A. Simulating the Formation of Surfactant-Templated Mesoporous Silica Materials: A Model with Both Surfactant Self-Assembly and Silica Polymerization. *Langmuir* **2013**, *29*, 766−780.
(39) Dellago, C.; Bolhuis, P.; Csajka, F.; Chandler, D. Transition Path Sampling and the Calculation of Rate Constants. *J. Chem. Phys.* **1998**, *108*, 1964−1977.
(40) Dellago, C.; Bolhuis, P.; Chandler, D. On the Calculation of Reaction Rate Constants in the Transition Path Ensemble. *J. Chem. Phys.* **1999**, *110*, 6617−6625.
(41) Allen, R.; Warren, P.; ten Wolde, P. Sampling Rare Switching Events in Biochemical Networks. *Phys. Rev. Lett.* **2005**, *94*, 018104.
(42) Allen, R.; Frenkel, D.; ten Wolde, P. Simulating Rare Events in Equilibrium or Nonequilibrium Stochastic Systems. *J. Chem. Phys.* **2006**, *124*, 024102.
(43) Agarwal, V.; Peters, B.; Rice, S. A.; Dinner, A. R. *Adv. Chem. Phys.* **2014**, *155*, 97−159.
(44) Earl, D.; Deem, M. Parallel Tempering: Theory, Applications, and New Perspectives. *Phys. Chem. Chem. Phys.* **2005**, *7*, 3910−3916.
(45) Swendsen, R.; Wang, J. Replica Monte-carlo Simulation of Spin-glasses. *Phys. Rev. Lett.* **1986**, *57*, 2607−2609.
(46) Jin, L.; Auerbach, S. M.; Monson, P. A. Emergence of Zeolite Analogs and other Microporous Crystals in an Atomic Lattice Model of Silica and Related Materials. *J. Phys. Chem. Lett.* **2012**, *3*, 761−765.
(47) Iler, R. *The Chemistry of Silica: Solubility, Polymerization, Colloid and Surface Properties, and Biochemistry*; John Wiley and Sons: New York, 1979.
(48) Jorge, M.; Auerbach, S. M.; Monson, P. A. Modeling Spontaneous Formation of Precursor Nanoparticles in Clear-Solution Zeolite Synthesis. *J. Am. Chem. Soc.* **2005**, *127*, 14388−14400.
(49) Catlow, C. R. A.; Ackermann, L.; Bell, R. G.; Cora, F.; Gay, D. H.; Nygren, M. A.; Pereira, J. C.; Sastre, G.; Slater, B.; Sinclair, P. E. Computer Modelling as a Technique in Solid State Chemistry - Introductory Lecture. *Faraday Discuss.* **1997**, *106*, 1−40.
(50) Demmelmaier, C. A.; White, R. E.; van Bokhoven, J. A.; Scott, S. L. Evidence for a Chromasiloxane Ring Size Effect in Phillips (Cr/SiO_2) Polymerization Catalysts. *J. Catal.* **2009**, *262*, 44−56.
(51) Rathore, N.; Chopra, M.; de Pablo, J. Optimal Allocation of Replicas in Parallel Tempering Simulations. *J. Chem. Phys.* **2005**, *122*, 024111.
(52) Metropolis, N.; Rosenbluth, A.; Rosenbluth, M.; Teller, A.; Teller, E. Equation of State Calculations by Fast Computing Machines. *J. Chem. Phys.* **1953**, *21*, 1087−1092.
(53) Zana, R.; Yeager, E. Ultrasonic Vibration Potentials in Tetraalkylammonium Halide Solutions. *J. Phys. Chem.* **1967**, *71*, 4241−4244.
(54) Le Roux, S.; Jund, P. Ring Statistics Analysis of Topological Networks: New Approach and Application to Amorphous Ges2 and SiO_2 Systems. *Comput. Mater. Sci.* **2010**, *49*, 70−83.
(55) Yuan, X.; Cormack, A. Efficient Algorithm for Primitive Ring Statistics in Topological Networks. *Comput. Mater. Sci.* **2002**, *24*, 343−360.
(56) Auerbach, S. M.; Carrado, K. A.; Dutta, P. K. *Handbook of Layered Materials*; Dekker: New York, 2004.

DOI: 10.1021/acs.jpcc.5b09450
J. Phys. Chem. C 2015, 119, 28046−28054